Comparative study of bandwidths in copper delafossites from x-ray emission spectroscopy

D. Shin,[1] J. S. Foord,[1] D. J. Payne,[1] T. Arnold,[1] D. J. Aston,[1] R. G. Egdell,[1,*] K. G. Godinho,[2] D. O. Scanlon,[2] B. J. Morgan,[2] G. W. Watson,[2] E. Mugnier,[3] C. Yaicle,[3] A. Rougier,[3] L. Colakerol,[4] P. A. Glans,[4] L. F. J. Piper,[4] and K. E. Smith[4]

[1]*Department of Chemistry, Chemistry Research Laboratory, University of Oxford, Mansfield Road, Oxford OX1 3TA, United Kingdom*

[2]*School of Chemistry, Trinity College Dublin, Dublin 2, Ireland*

[3]*Laboratoire de Réactivité et de Chimie des Solides, CNRS UMR-6007, Université de Picardie Jules Verne, 33 rue Saint Leu, 80039 Amiens Cedex, France*

[4]*Department of Physics, Boston University, 590 Commonwealth Avenue, Boston, Massachusetts 02215, USA*

(Received 3 November 2009; published 30 December 2009)

The widths of the valence bands in the copper (I) delafossites $CuGaO_2$, $CuInO_2$, and $CuScO_2$ have been measured by O *K*-shell x-ray emission spectroscopy and are compared with previous experimental work on $CuAlO_2$ and $CuCrO_2$. In agreement with recent density-functional theory calculations it is found that the bandwidth decreases in the series $CuAlO_2 > CuGaO_2 > CuInO_2 > CuScO_2$. It is shown that states at the top of the valence band are of dominant Cu $3d_{z^2}$ atomic character but with significant mixing with O $2p$ states.

DOI: 10.1103/PhysRevB.80.233105 PACS number(s): 73.20.At, 73.43.Cd, 78.70.En

Widespread interest in the electronic properties of ternary delafossite oxides of Cu^I with the general formula $Cu^I T^{III} O_2$ (where T^{III} is a trivalent metal ion) has been prompted by the fact that these materials combine the properties of optical transparency in the visible region with a reasonable *p*-type conductivity. This leads to potential applications in "transparent oxide electronics" where the *p*-type delafossite is combined with an *n*-type transparent conducting oxide (TCO) to give a transparent *p*-*n* junction.[1,2] The first *p*-type TCO to attract attention was $CuAlO_2$,[3,4] followed later by $CuGaO_2$ (Ref. 5) and $CuInO_2$.[6,7] The last of these compounds is of particular interest as it is amenable to bipolar doping. More recently $CuScO_2$ (Ref. 8) and $CuCrO_2$ (Refs. 9–12) have emerged as alternative *p*-type TCOs: the highest conductivity in any *p*-type TCO is found in Mg-doped $CuCrO_2$.[9] Somewhat surprisingly the optically measured band gaps in the group 13 delafossites follow the sequence $CuAlO_2(3.5\ \text{eV}) < CuGaO_2(3.6\ \text{eV}) < CuInO_2(3.9\ \text{eV})$:[13] this order is opposite to that seen in binary oxides and nitrides of this group. By contrast a "conventional" evolution of measured optical gaps is found in the group 3 series $CuScO_2(3.7\ \text{eV}) > CuYO_2(3.5\ \text{eV}) > CuLaO_2(2.4\ \text{eV})$.[13] The puzzling trend in group 13 has been explained in terms of a large difference between the lowest-energy gap and the onset of strong optical absorption. This arises in part because the lowest-energy band gaps are indirect but in addition the values for direct transition dipole matrix elements from states at the top of the valence band into the conduction band are either zero or very low over a wide range of energies, which is bigger for $CuInO_2$ than for $CuAlO_2$.[14] A similar delayed optical onset has recently been established in the *n*-type TCO In_2O_3 on the basis of a comparison between density-functional theory (DFT) calculations and x-ray photoemission and O *K*-edge x-ray emission measurements.[15] More recent theoretical calculations show that the difference between direct and indirect gaps is bigger in group 13 than in group 3, thus explaining the differing trends in the two groups.[13]

Within the delafossite structure each Cu atom is linearly coordinated by two oxygen atoms, forming O-Cu-O dumbbells parallel to the *c* axis. The oxygen atoms that terminate the dumbbells are also each coordinated to three T atoms, oriented such that T-centered octahedra form AlO_2 layers which lie parallel to the *ab* plane. Two alternative layer stacking sequences *ABABAB* and *ABCABC* are possible to give hexagonal (space group $P6_3/mmc$) (Ref. 16) or rhombohedral (space group $R3\bar{m}$) (Ref. 17) polymorphs, respectively. Within the linear O-Cu-O units the Cu $3d_{z^2}$ orbitals have σ-like symmetry, the Cu $3d_{xz}$ and $3d_{yz}$ orbitals π-like symmetry and the Cu $3d_{xy}$ and Cu $3d_{x^2-y^2}$ orbitals δ-like symmetry. No mixing with O $2p$ states is possible for the Cu $3d$ orbitals of δ symmetry.[18] Linear coordination about copper is also found in the binary oxide Cu_2O. However the band gap in the parent material has a much smaller value of 2.17 eV than in delafossites.[19] The difference is attributed to the fact that Cu has 12 Cu next nearest neighbors in Cu_2O, whereas there are only six coplanar next-nearest neighbors in the delafossite structure. This leads to a reduction in the Cu $3d$ bandwidth and a wider band gap.

Very recent calculations predict that the widths of the occupied valence bands in Cu delafossites should follow the order $CuAlO_2 > CuGaO_2 > CuInO_2 > CuScO_2$.[20] Valence bandwidths in $CuAlO_2$ (Ref. 21) and $CuCrO_2$ (Refs. 22 and 23) have been measured by x-ray photoemission spectroscopy (XPS) and x-ray emission spectroscopy (XES) but to date there has been no comparable experimental work on $CuGaO_2$ and $CuInO_2$. In the present Brief Report we present O *K*-edge x-ray emission spectra of $CuGaO_2$ and $CuInO_2$. Taken in conjunction with the previous work on $CuAlO_2$ our results establish that the experimental bandwidths in the group 13 delafossites do indeed fall in the order predicted by theory. The work is extended to include measurements on $CuScO_2$ which transpires to have a narrower valence band than any of the main group compounds. We also present valence-band XPS data for $CuInO_2$. Comparison between XPS and XES allow us to establish that as for $CuAlO_2$ and $CuCrO_2$, the upper part of the valence band is composed of states of dominant Cu $3d$ atomic character whereas states in the bottom half of the valence band have dominant O $2p$ character.

$CuGaO_2$ was prepared by firing a finely ground mixture of

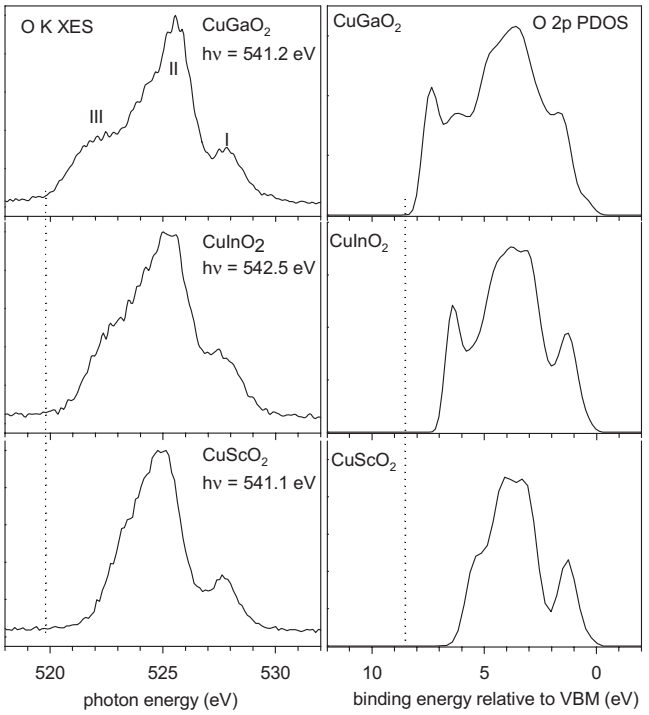

FIG. 1. Left-hand panels: O *K*-shell x-ray emission spectra of 3R-$CuGaO_2$, 3R-$CuInO_2$ and 2H-$CuScO_2$. Right-hand panels: O 2*p* partial densities of states for the same three materials adapted from Ref. 20.

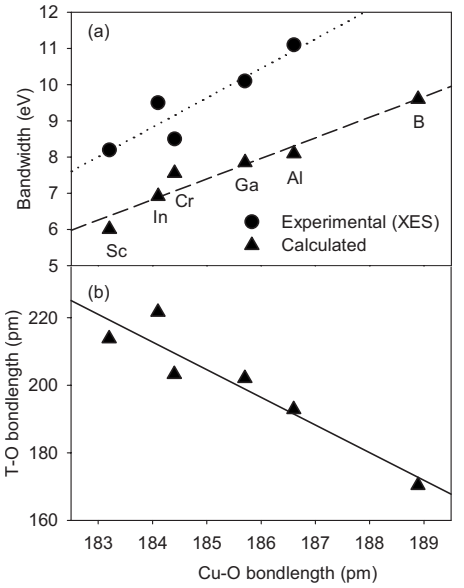

FIG. 2. (a) Comparison between measured bandwidths and Cu-O bond lengths calculated by generalized gradient approximation density-functional theory. Experimental data for $CuGaO_2$, $CuInO_2$, and $CuScO_2$ from present work, calculated values from Ref. 20. Experimental and calculated values for $CuAlO_2$ and $CuCrO_2$ from Refs. 21–23. Calculated value for $CuBO_2$ from Ref. 26. (b) Plot illustrating the inverse correlation between Cu-O and T-O bond lengths.

Ga_2O_3 (Aldrich 99.99%) and Cu_2O (Aldrich 99.99%) under flowing argon at 1100 °C for 24 h. The sample was then pressed into pellets between tungsten carbide dies and refired as above for a further 24 h. The x-ray diffraction pattern of the product was characteristic of the 3R phase. $CuScO_2$ was prepared by firing a pelletized mixture of CuO and Sc_2O_3 in air at 1100 °C for 24 h, followed repelletization and refiring at 1100 °C for a further 24 h. The samples were quenched from 1100 °C by dropping into liquid nitrogen to prevent oxidation. Phase pure 2H material was obtained by using a 1% excess of CuO, as described by Kykyneshi *et al.*[24] $CuInO_2$ was prepared by pulsed laser deposition from a $Cu_2In_2O_5$ target under an oxygen ambient with $p_{O_2}=5\times10^{-3}$ mbar, as described in detail elsewhere.[25] Samples for the photoemission study were prepared using a low level (2%) of Eu doping, which helped eliminate problems due to sample charging. High-resolution Al $K\alpha$ x-ray photoemission spectra excited at $h\nu=1486.6$ eV were measured in a Scienta ESCA 300 spectrometer. The effective instrument resolution was 400 meV. Samples were cleaned *in situ* by annealing at 400 °C which reduced the C 1*s* to O 1*s* intensity ratio to below 1/100. Binding energies are referenced to the Fermi energy of a silver sample regularly used to calibrate the spectrometer.

X-ray emission spectra were measured on beamline 7.0.1 at the Advanced Light Source (ALS), Lawrence Berkeley National Laboratory. This beamline is equipped with a spherical grating monochromator. Emission spectra were recorded using a Nordgren-type grazing-incidence spherical grating spectrometer. The beamline was set to have an energy resolution of 500 meV at the O *K* edge and the emission spectrometer was set to have a resolution of 350 meV. The O *K* emission spectra were calibrated relative to Zn $L_{1,2}$ emission lines of Zn metal in second order.

O *K*-shell x-ray emission spectra of $CuGaO_2$, $CuInO_2$, and $CuScO_2$ are shown in the left-hand panels of Fig. 1: the right-hand panels show the corresponding O 2*p* partial densities of states (DOSs) derived from density-functional theory calculations. Decay of the O 1*s* core hole is governed by a strict dipole selection rule which only allows transitions from states with O 2*p* character. Thus the spectra provide a faithful measure of the O 2*p* partial density of states. In each case the spectra are dominated by a strong central peak labeled II in the figure with weaker features I and III to high and low photon energy, respectively. It can be clearly seen that there is a progressive decrease in the width of the valence band in the experimental spectra following the sequence $CuGaO_2>CuInO_2>CuScO_2$. The available experimental data for the delafossites are summarized in Fig. 2(a) where the experimental bandwidths are compared with results from density-functional theory calculations. The figure also include the calculated bandwidth for $CuBO_2$.[26] There is very good qualitative agreement between theory and experiment although the measured bandwidths are systematically bigger than in the calculations. Discrepancies of this type are a well-known problem when comparing the results of DFT with experimental data. Somewhat surprisingly there is a direct (rather than inverse) correlation between the overall width of the valence band and the calculated Cu-O bond length. However as shown in Fig. 2(b) there is an inverse correlation between the Cu-O and T-O bond lengths and the bandwidth therefore increases as the T-O bonds become shorter.

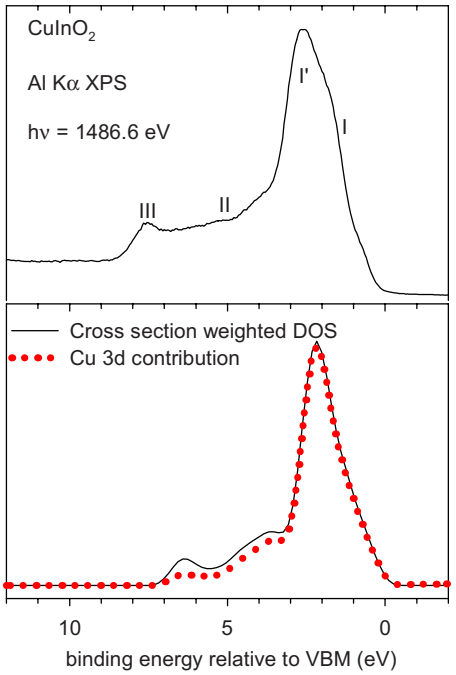

FIG. 3. (Color online) (a) Valence-band XPS of 2% Eu-doped $CuInO_2$. (b) Solid line: cross-section weighted density of states derived from band-structure calculations of reference. Dotted line: Cu 3*d* contribution to the cross-section weighted density of states.

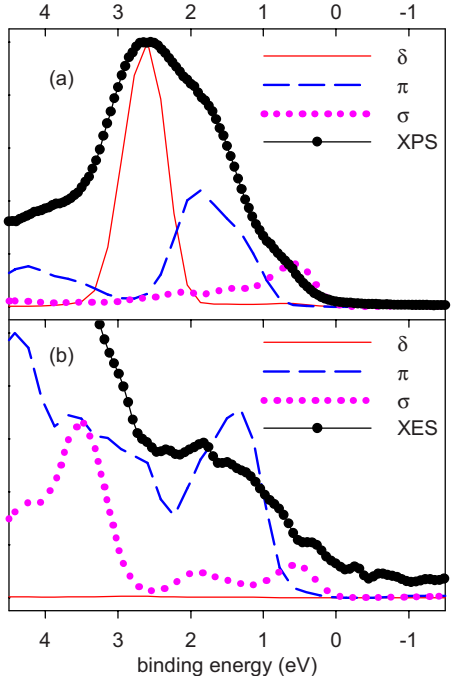

FIG. 4. (Color online) (a) The Cu PDOS in $CuInO_2$ decomposed into components with δ, π, and σ symmetry with respect the linear axis of the O-Cu-O dumbbells compared with Al $K\alpha$ XPS. The energy scale for the calculated DOS is multiplied by a factor of 1.2 to match the position of the peak in the δ component with that observed experimentally. Theoretical data adapted from Ref. 20. (b) Comparison between decomposed O PDOS and O *K*-edge XES along the same lines as in (a).

The pattern of intensities found in the x-ray emission spectra changes completely in x-ray photoemission spectra as seen in Fig. 3, where data for $CuInO_2$ are presented: the other delafossites showed very similar changes and the data are not presented here. The maximum intensity is now found at the top of the valence band with the peak about 2.7 eV below the band edge. This does not correspond to the maximum of peak I in the x-ray emission spectrum where the peak is found about 1.9 eV below the Fermi energy. We therefore label the peak maximum in XPS as I′: the structure corresponding to the XES peak appears as a low binding energy shoulder to this peak. The intensity changes arise because XPS is determined by the cross-section weighted density of states that is a sum of atomically projected partial densities of states with each contribution weighted by a one electron ionization cross section. The total density of states is derived mainly by contributions from O 2*p* and Cu 3*d* states but the cross section for ionization of Cu 3*d* states with Al $K\alpha$ radiation is a factor of 20 bigger than the O 2*p* cross section.[27] Thus the overall photoemission is dominated by the Cu 3*d* contribution, as shown in the lower panel to Fig. 3. The changes between XES and XPS thus demonstrate that the states in the upper part of the valence band which give rise to peaks I and I′ are of dominant Cu 3*d* character, whereas the states in the bottom half of the valence band associated with II and III are of dominant O 2*p* character. The nonvanishing intensity of I in O *K*-edge x-ray emission spectroscopy is a direct consequence of hybridization between Cu 3*d* and O 2*p* states arising from σ and π overlap within the O-Cu-O dumbbells. Conversely most of the intensity of peaks II and III in XPS arises not from the O 2*p* states themselves but from the hybridization of Cu 3*d* states with O 2*p* states in the bottom half of the valence band. The energy shift between peaks I and I′ arises from the fact that the latter is associated with nonbonding Cu 3*d* states of δ symmetry within the linear O-Cu-O units. Unlike the σ and π states, the δ states cannot hybridize with O 2*p* states[18,28] and so do not appear in XES. These ideas are illustrated in Fig. 4 where the Cu and O partial densities of states in the top half of the valence band are decomposed into components with local δ, π, and σ symmetry.[20] The peak maximum in XPS coincides with Cu δ states and π and σ states appear as low binding-energy shoulders. By contrast there is near zero O δ amplitude across the whole of the valence band.

In summary we have used new XES measurements to compare bandwidths in the delafossite oxides $CuGaO_2$, $CuInO_2$, and $CuScO_2$ with that in $CuAlO_2$. The overall sequence we have found is $CuAlO_2 > CuGaO_2 > CuInO_2 > CuScO_2$, in agreement with recent calculations.[20] The direct correlation between bandwidth and Cu-O bond length is found despite the fact that π interactions are stronger the shorter the bond and the separation between O $2p_{x/y}$ states and Cu $3d_{xz/yz}$ states is greatest in $CuScO_2$. However in the main group delafossites the position of the bottom of the valence band is determined by hybridization with valence *s* states of the group 13 element and the extent of this hybridization decreases on descending the group. This reduces the competition with hybridization between Cu 3*d* and O 2*p* σ states, allowing the Cu-O bond to contract but at the same time leading to a reduction in the overall width of the va-

lence band. There is very little contribution from Sc 4*s* states in $CuScO_2$ and the valence band is narrow. The increase in Cu-O bond length in moving across the transition series to $CuCrO_2$ arises from pronounced hybridization between Cr 3*d* and O 2*p* states across the entire valence band in this compound.

Experimental work on transparent conducting oxides in Oxford was supported under EPSRC under Grant No. GR/S94148 and the Scienta XPS facility by EPSRC under Grant No. EP/E025722/1. The Boston University program is supported in part by the U.S. Department of Energy under Grant No. DE-FG02-98ER45680 and in part by the Donors of the American Chemical Society Petroleum Research Fund. The Advanced Light Source is supported by the Director, Office of Science, Office of Basic Energy Sciences, of the U.S. Department of Energy under Contract No. DE-AC02-05CH11231. Theoretical work in TCD is funded by Science Foundation Ireland under PI Grants No. 06/IN.1/I92 and No. 06/IN.1/I92/EC07. D.S. is grateful to the Korea Industrial Technology Foundation (KOTEF) for support.

*Corresponding author; russell.egdell@chem.ox.ac.uk

[1] H. Kawazoe, H. Yanagi, K. Ueda, and H. Hosono, MRS Bull. **25**, 28 (2000).
[2] K. Tonooka and N. Kikuchi, Thin Solid Films **515**, 2415 (2006).
[3] H. Kawazoe, M. Yasukawa, H. Hyodo, M. Kurita, H. Yanagi, and H. Hosono, Nature (London) **389**, 939 (1997).
[4] H. Yanagi, S. Inoue, K. Ueda, H. Kawazoe, H. Hosono, and N. Hamada, J. Appl. Phys. **88**, 4159 (2000).
[5] K. Ueda, T. Hase, H. Yanagi, H. Kawazoe, H. Hosono, H. Ohta, M. Orita, and M. Hirano, J. Appl. Phys. **89**, 1790 (2001).
[6] H. Yanagi, T. Hase, S. Ibuki, K. Ueda, and H. Hosono, Appl. Phys. Lett. **78**, 1583 (2001).
[7] H. Yanagi, K. Ueda, H. Ohta, M. Orita, M. Hirano, and H. Hosono, Solid State Commun. **121**, 15 (2002).
[8] Y. Kakehi, K. Satoh, T. Yotsuya, K. Masuko, T. Yoshimura, A. Ashida, and N. Fujimura, J. Cryst. Growth **311**, 1117 (2009).
[9] R. Nagarajan, A. D. Draeseke, A. W. Sleight, and J. Tate, J. Appl. Phys. **89**, 8022 (2001).
[10] S. Mahapatra and S. A. Shivashankar, Chem. Vap. Deposition **9**, 238 (2003).
[11] D. Li, X. D. Fang, Z. H. Deng, S. Zhou, R. H. Tao, W. W. Dong, T. Wang, Y. P. Zhao, G. Meng, and X. B. Zhu, J. Phys. D **40**, 4910 (2007).
[12] M. Poienar, F. Damay, C. Martin, V. Hardy, A. Maignan, and G. Andre, Phys. Rev. B **79**, 014412 (2009).
[13] M. N. Huda, Y. F. Yan, A. Walsh, S. H. Wei, and M. M. Al-Jassim, Phys. Rev. B **80**, 035205 (2009).
[14] X. L. Nie, S. H. Wei, and S. B. Zhang, Phys. Rev. Lett. **88**, 066405 (2002).
[15] A. Walsh *et al.*, Phys. Rev. Lett. **100**, 167402 (2008).
[16] O. Crottaz and F. Kubel, Z. Kristallogr. **211**, 481 (1996).
[17] O. Crottaz and F. Kubel, Z. Kristallogr. **211**, 482 (1996).
[18] P. Marksteiner, P. Blaha, and K. Schwarz, Z. Phys. B: Condens. Matter **64**, 119 (1986).
[19] S. Nikitine, J. B. Grun, and M. Sieskind, J. Phys. Chem. Solids **17**, 292 (1961).
[20] K. G. Godhino, D. O. Scanlon, B. J. Morgan, and G. W. Watson (unpublished).
[21] D. J. Aston, D. J. Payne, A. J. H. Green, R. G. Egdell, D. S. L. Law, J. Guo, P. A. Glans, T. Learmonth, and K. E. Smith, Phys. Rev. B **72**, 195115 (2005).
[22] D. O. Scanlon, A. Walsh, B. J. Morgan, G. W. Watson, D. J. Payne, and R. G. Egdell, Phys. Rev. B **79**, 035101 (2009).
[23] T. Arnold, D. J. Payne, A. Bourlange, J. P. Hu, R. G. Egdell, L. F. J. Piper, L. Colakerol, A. De Masi, P. A. Glans, T. Learmonth, K. E. Smith, J. Guo, D. O. Scanlon, A. Walsh, B. J. Morgan, and G. W. Watson, Phys. Rev. B **79**, 075102 (2009).
[24] R. Kykyneshi, B. C. Nielsen, J. Tate, J. Li, and A. W. Sleight, J. Appl. Phys. **96**, 6188 (2004).
[25] C. Yaicle, A. Blacklocks, A. V. Chadwick, J. Perriere, and A. Rougier, Appl. Surf. Sci. **254**, 1343 (2007).
[26] D. O. Scanlon, A. Walsh, and G. W. Watson, Chem. Mater. **21**, 4568 (2009).
[27] J. J. Yeh and I. Lindau, At. Data Nucl. Data Tables **32**, 1 (1985).
[28] J. P. Hu, D. J. Payne, R. G. Egdell, P. A. Glans, T. Learmonth, K. E. Smith, J. Guo, and N. M. Harrison, Phys. Rev. B **77**, 155115 (2008).